

**Photoacoustic determination of radiative quantum efficiency of surface plasmons in silver films**

T. Inagaki and Y. Nakagawa

*Department of Physics, Osaka Kyoiku University, Tennoji, Osaka 543, Japan*

E. T. Arakawa and D. J. Aas\*

*Health and Safety Research Division, Oak Ridge National Laboratory, Oak Ridge, Tennessee 37830*

(Received 6 July 1982)

Total light scattering from thin silver films in an attenuated-total-reflection geometry was determined as a function of the angle of incidence of 1.96-eV photons by using a combination of photoacoustic and optical measurements. From the results obtained at the plasmon resonance angle, the quantum efficiency of light emission from surface plasmons was determined as a function of film thickness and roughness. The thickness-dependent results, analyzed by the use of a Gaussian roughness spectrum, were found to be consistent with the predictions of Kröger and Kretschmann's theory for light scattering from rough thin films at all angles of incidence. From the values of the roughness parameters determined, the quantum efficiencies of light emission from the prism and the air sides of the silver film were evaluated as functions of film thickness.

**I. INTRODUCTION**

Resonant excitation and relaxation of surface plasmons in metals have continued to attract a great deal of attention. Recently, we have reported<sup>1,2</sup> the first experimental results of the direct observation of nonradiative relaxation of surface plasmons in a thin silver film. This observation was made by illuminating an attenuated-total-reflection ATR photon-plasmon coupler attached to a sealed gas-filled cell by a chopped monochromatic photon beam. Absorption of *p*-polarized photons in the thin silver film due to plasmon excitation produced a periodic heat generation through nonradiative relaxation of the excited surface plasmons, and the subsequent heat flow from the film to the gas caused a periodic pressure variation in the cell, which was detected by a microphone exposed to the gas. Our photoacoustic<sup>3</sup> method was thus capable of probing directly nonradiative relaxations of surface plasmons occurring in the thin silver film.

Nonradiative surface plasmons excited on a planar metal surface by the ATR method in either the Kretschmann<sup>4</sup> (prism-film-air) or the Otto<sup>5</sup> (prism-air-metal) geometries have both radiative and nonradiative decay channels.<sup>6</sup> The plasmons can decay by emitting photons into the prism through which photons were incident to excite the plasmons. This radiative decay of nonradiative surface plasmons into the prism is just the reverse process of plasmon excitation, and the decay rate is

known to depend strongly on the film thickness in the Kretschmann geometry or on the thickness of the air gap in the Otto geometry. In cases of very thin films or air gaps, this radiative relaxation is indeed the predominant factor which determines the halfwidth of the spectral shape of the plasmon resonance. However, in order to conserve momentum upon decay into photons, photons from this mode of decay are emitted only in the direction of the specular reflection of the incident light and are thus superimposed on the reflected light.

The presence of roughness on the metal surface opens two additional channels of radiative decay,<sup>6</sup> which result in light emission in directions other than specular. One is for plasmons scattered with momentum unchanged, and the other is for plasmons whose momentum values are decreased upon scattering by the surface roughness. The former plasmons can decay into the prism as photons by the same mechanism as plasmons on a planar surface and are known<sup>7,8</sup> to form a hollow cone of scattered light with a half-angle equal to the plasmon resonance angle. The latter plasmons may decay radiatively into the prism and also from the air side of the metal film in the Kretschmann geometry if the momenta of the scattered plasmons are smaller than that of the photons in air. Because of the relative ease of experimental observation, this latter radiative process from the air side of the film has been studied extensively<sup>6</sup> and has been used to obtain information on the properties of rough sur-

faces. The remaining plasmons, scattered or unscattered, are absorbed internally in the metal itself. This creates single-electron excited states in the metal which relax nonradiatively and eventually degrade into quanta of lattice energy which can be detected photoacoustically.

The photoacoustic technique when used as a probe of nonradiative relaxation of excited states in matter provides a new way of obtaining information which is difficult to study by conventional experimental methods. In the previous paper,<sup>1,2</sup> we have demonstrated that the photoacoustic signal generated from an ATR system in the Kretschmann geometry gives direct information concerning the quantum efficiency of light emission from surface plasmons. As was described above, the photoacoustic signal probes surface plasmons which undergo nonradiative relaxation, while the total number of surface plasmons which are excited in a thin metal film is known from the total photon energy absorbed. Therefore, the relative number of surface plasmons which decay radiatively by emitting photons may be determined from the difference of the photoacoustic signal from the optical absorptance, if the former is properly normalized to the latter using the response constant of the photoacoustic cell. We were thus able<sup>1,2</sup> to separate the radiatively and nonradiatively decaying surface plasmons and to determine the radiative quantum efficiency of surface plasmons, defined by the number of photons emitted divided by the number of plasmons excited. In one particular sample, the radiative quantum efficiency was found to be roughly 0.3 for a 34-nm-thick silver film.<sup>2</sup>

In this paper, we have applied the same photoacoustic technique to a series of thin silver films of variable thickness and roughness and determined the total light scattering from these films as a function of the angle of photon incidence. From the results obtained at the plasmon resonance angle, we determined the quantum efficiency for roughness-aided light emission from surface plasmons as a function of film thickness and roughness. These experimental results were analyzed by using Kröger and Kretschmann's first-order light-scattering theory<sup>9</sup> for a rough thin film.

Recently, Moreland *et al.*<sup>10</sup> have determined the quantum efficiency of light emission from the air side of silver films by direct measurement of the emitted light intensity. For films of thicknesses between 20 and 70 nm they found the efficiencies for 1.96-eV photons to be  $0.05 \pm 0.02$  with no strong dependence on the film thickness. On the other

hand, a similar measurement by Simon and Guha<sup>7</sup> some years ago on the prism side of a 55-nm-thick silver film gave an efficiency of  $\leq 0.001$ . Both results should depend strongly on film roughness and the latter also on film thickness. The present photoacoustic experiments give systematic results of the sum of these quantum efficiencies as functions of film thickness and roughness.

## II. EXPERIMENT

The ATR photon-plasmon coupler equipped with a photoacoustic cell was essentially the same as that used in the previous study.<sup>1,2</sup> In the present study we have used six identical air-filled photoacoustic cells, three to a cell frame. This allowed us to study three different silver samples made in the same evaporation. The films of silver were evaporated at  $5 \times 10^{-6}$  Torr onto the hypotenuse surface of a strain-free 45° glass prism, and the thickness and deposition rate ( $\sim 1$  nm/sec) were monitored by a quartz-crystal oscillator. Rough silver films were made by evaporating silver onto a CaF<sub>2</sub> underlayer which had been evaporated on a glass prism under similar evaporation conditions.

A cell frame with three photoacoustic cells was set on the prism in a manner described previously.<sup>1,2</sup> The area of each cell which covered the film sample was  $2 \times 10$  mm<sup>2</sup>, and the thickness of the air-filled cavity formed above the film was 1 mm. This thickness was sufficiently larger than the thermal diffusion length of air at the chopping frequency of the incident light used in the present study that the ordinary one-dimensional theories<sup>11,12</sup> for photoacoustic signal generation from solids were applicable to the data taken with these cells. Prior to placement on the prism coupler, all the cells were checked for a linear photoacoustic response to the incident power. Checks were also made on the cells to ensure that the signal was independent of the position where the incident light hit the film sample due to changing the angle of incidence.

The prism coupler attached to the photoacoustic cells was placed on a rotatable platform and illuminated by a chopped parallel beam of *p*-polarized 1.96-eV photons from a 1-mW He-Ne laser. The photoacoustic signal was measured at a chopping frequency of 300 Hz as a function of the angle of incidence. The signal measured at each angle of incidence was corrected for small fluctuations of the incident-light intensity and for the reflection loss of the incident-light intensity at the prism-

entrance surface. The results were then corrected for the signal generation by the light which was reflected back from the prism-exit surface. Finally, they were normalized, for comparison purposes, for the small differences in the response constants of the photoacoustic cells used. The relative values of the response constants for the cells were determined by measuring the photoacoustic signals from the same silver film. The experimental data presented in the next section are these corrected and normalized results.

Simultaneously with the photoacoustic measurements described above, the photon intensities both reflected from and transmitted through the prism coupler were measured at each angle of incidence, together with the incident-light intensity, by using a photoacoustic photon detector, the details of which were described previously.<sup>1,2</sup> After being corrected for the reflection losses at the prism and the cell-window surfaces, these data were used to determine the reflectance  $R$  and the transmittance  $T$  for the two-boundary system of glass-silver-air, from which the absorptance  $A$  in the silver film was determined as a function of the angle of incidence. The photoacoustic photon detector used in the present experiment was about 10 times more sensitive than that used in the previous experiment. The stability of the He-Ne laser used as a light source was also improved during the course of the experiment. The experimental accuracies of both the absorptance and photoacoustic data as compared with our previous experiments<sup>1,2</sup> were thus improved significantly.

### III. EXPERIMENTAL RESULTS AND ANALYSES

#### A. Silver films of variable thickness

An example of a set of our experimental results of  $R$ ,  $T$ , and the photoacoustic signal taken with a 24-nm-thick silver film is presented in Fig. 1 as a function of the angle of incidence  $\phi$ . Typical experimental uncertainties are indicated in the figure.  $T$  at angles just below the critical angle (41.30°) for total reflection at the prism-air interface was not measured because the cell frame interfered with the transmitted photon beam, while at angles above the critical angle no light was transmitted.  $R$  exhibits the well-known dip due to plasmon excitation just above the critical angle, indicating that in this case about 70% of the incident photons were converted into surface plasmons. Corresponding to this structure in  $R$ , a strong enhancement of the photoacous-

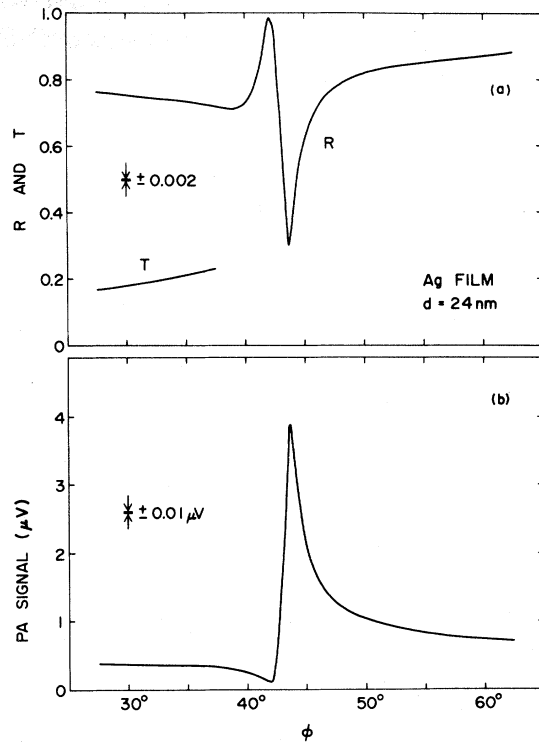


FIG. 1. (a) Reflectance  $R$  and transmittance  $T$  and (b) photoacoustic signal for a 24-nm-thick silver film obtained with  $p$ -polarized 1.96-eV photons as a function of the angle of incidence  $\phi$ .

tic signal, which demonstrates nonradiative degradation of the excited plasmons into heat, is seen to occur at the same angle of photon incidence.

In the previous study,<sup>2</sup> we showed by using the theory<sup>11</sup> for the generation of photoacoustic signals from solids that if the excited states created in the silver film relax only through nonradiative processes, our ATR photoacoustic system gives a signal amplitude which is proportional to the total photon energy absorbed, or to the absorptance, at any angle of incidence. This was predicted from the thermal properties and the densities of glass, silver, and air (the component materials of our photoacoustic system), and the optical properties of the silver films and their thickness range, by using the fact that the relaxations of excited states in silver, including surface plasmons, may be considered to be instantaneous at the chopping frequency and photon energy employed. Any difference between the photoacoustic and absorptance data as a function of the angle of incidence may therefore be considered to be due to radiative decay processes occurring in the silver film.

Keeping this in mind, we present in Fig. 2 the results of the absorptances  $A$  ( $=1-R-T$ ) for three films of different thicknesses made in the same evaporation and compare them with their respective photoacoustic signals as a function of the angle of incidence. The resemblance between these two sets of data for each film is evident in the figure. As the film thickness increases, the halfwidth of the plasmon structure in  $A$  decreases, and the angle at which the plasmon peak occurs becomes smaller. The same behavior is seen in the plasmon structure in the photoacoustic data. The relative peak height as a function of the film thickness is also similar in both data. Such an overall agreement between the photoacoustic and the absorptance data indicates that the decay processes occurring in our silver films are primarily nonradiative. However, a careful quantitative comparison shows evidence for a systematic contribution due to radiative processes.

A quantitative comparison was made by normalizing the photoacoustic data to the absorptance data in the range of angles below the critical angle. For these angles of incidence it is not possible to excite surface plasmons on a planar silver film, and the

excited states created by 1.96-eV photons are single-electron intraband excited states of the Drude type which relax through nonradiative processes. Since this photon energy is considerably smaller than the work function of silver,<sup>1,2</sup> the possibility of photoelectron emission from the excited states may also be ignored. Thus, below the critical angle, no part of the absorbed energy can escape from the film as reradiated photons or photoelectrons, and all the absorbed energy should be dissipated in the film. The normalization constants, defined by the absorptance divided by the photoacoustic signal amplitude, were calculated for films of various thicknesses from the experimental data below the critical angle, and the results are plotted in Fig. 3 as a function of film thickness  $d$ . The values calculated at different angles of incidence agreed well with each other within the experimental uncertainty indicated by the error bars in the figure. The normalization constant should be independent of the film thickness, but it was found to decrease slightly with increasing film thickness, tending to a constant value at large thicknesses. We attributed this to the contribution from light scattering from the silver film which becomes appreciably larger as the film becomes thinner. The value of the normalization constant due to actual light absorption in the silver films was chosen to be  $0.142 \mu\text{V}^{-1}$  (the asymptotic value at large thicknesses indicated by a dashed line in the figure), and deviations of the normalization constant from this value were attributed to light scattering from the silver films. The light scatter-

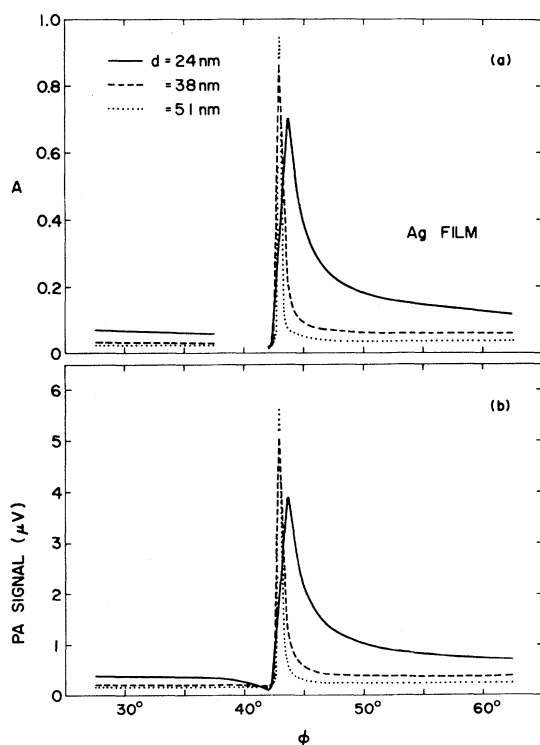


FIG. 2. (a) Absorptances  $A$  and (b) photoacoustic signal amplitudes for silver films of different thicknesses  $d$  obtained with  $p$ -polarized 1.96-eV photons as a function of the angle of incidence  $\phi$ .

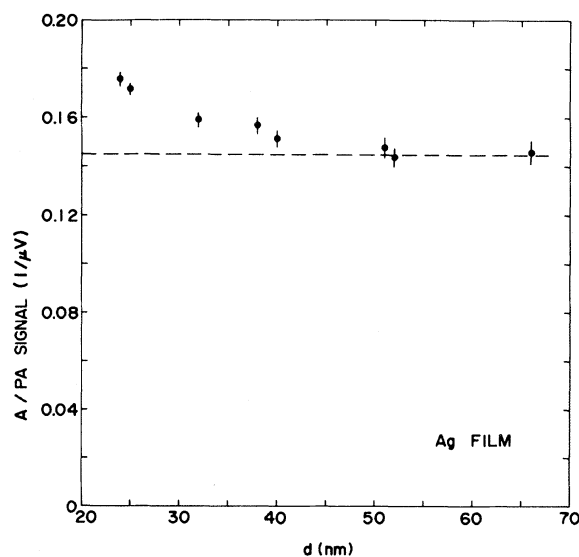


FIG. 3. Normalization constant as a function of film thickness  $d$ .

ing,  $A_{sc}$ , relative to the incident intensity was thus evaluated at  $\phi = 30^\circ$  from the observed absorbance values  $A$  at each film thickness. The validity of this interpretation was then checked by comparing these estimated values of  $A_{sc}$  with theoretical values calculated from Kröger and Kretschmann's theory<sup>9</sup> for light scattering from rough thin films. Such a comparison is made in Fig. 4, in which it is seen that the estimated values of  $A_{sc}$  exhibit reasonable agreement with the theoretical values which were calculated by using the values of the roughness parameters determined from the experimental results of the radiative quantum efficiency and the light scattering presented below. We will give details of the theoretical calculation of  $A_{sc}$  and return to the results in Fig. 4 in the next section.

The photoacoustic data for a 24-nm-thick film in Fig. 1 was normalized to the absorbance by using the normalization constant thus determined, and the result is presented in Fig. 5 as a function of the angle of incidence, together with the absorbance data. As is expected, the normalized signal  $\bar{S}_{pa}$  is smaller than the observed absorbance  $A$  at all angles of incidence. From the arguments already given above, the difference  $(A - \bar{S}_{pa})$  at each angle of incidence may be considered to be due to radiative processes and represents the fraction of the incident intensity which was reradiated from the silver film. In other words, the difference  $(A - \bar{S}_{pa})$  represents the total light-scattering intensity divided by the incident intensity. On the other hand,  $\bar{S}_{pa}$

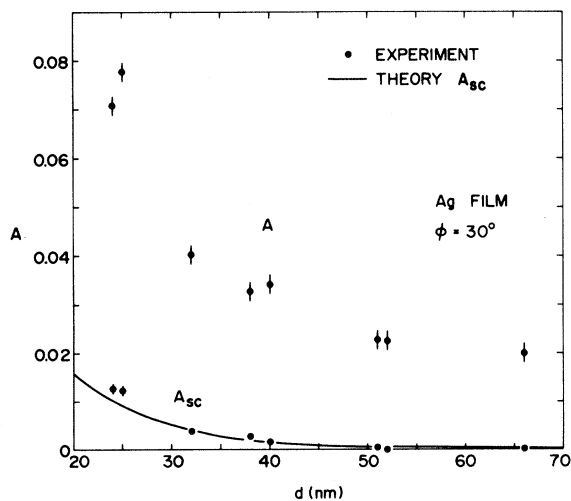


FIG. 4. Observed absorbance  $A$  and evaluated contribution  $A_{sc}$  from light scattering at the angle of incidence  $\phi = 30^\circ$  as a function of film thickness  $d$ . Solid line represents the result for  $A_{sc}$  calculated from Kröger and Kretschmann's theory.

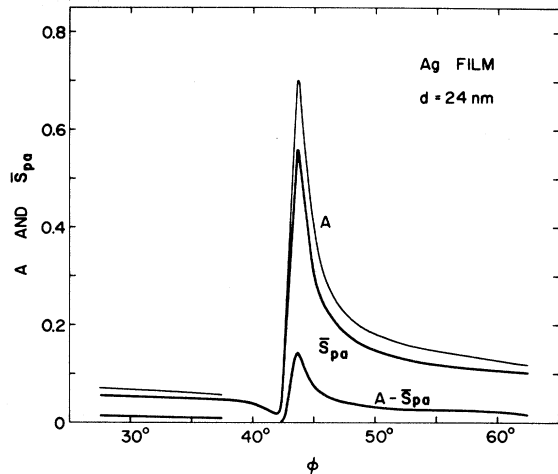


FIG. 5. Comparison between absorbance  $A$  and normalized photoacoustic signal  $\bar{S}_{pa}$  as a function of the angle of incidence  $\phi$ .

represents the fraction of the incident intensity which was dissipated in the film and generated the photoacoustic signal. The photons absorbed at each angle of incidence were thus divided into two groups—reradiated and dissipated—and the radiative and nonradiative quantum efficiencies are given by  $(A - \bar{S}_{pa})/A$  and  $\bar{S}_{pa}/A$ , respectively.

The total light scattering  $(A - \bar{S}_{pa})$  from a 24-nm-thick film determined in Fig. 5 as a function of the angle of incidence exhibits a plasmon resonance structure, corresponding to emission of the well-known plasmon radiation. The values of  $A - \bar{S}_{pa}$  obtained for three films of different thicknesses made in the same evaporation is presented in Fig. 6. It is seen that the scattering intensity at the angles outside the resonance region decreases rapidly with increasing film thickness, while the intensity at the resonance angle varies only slightly with film thickness. The sharp profile of the resonance structure obtained for the 51-nm-thick film is similar to ones observed by direct measurement of the scattered-light intensity from the air side of the films by a number of authors<sup>13</sup> for relatively thick silver films, and the broad profile obtained for the 24-nm-thick film resembles one observed recently by Hayashi *et al.*<sup>14</sup> for a silver film of comparable thickness.

From the results of the total light scattering in Fig. 6, the radiative quantum efficiencies  $(A - \bar{S}_{pa})/A$  at the plasmon resonance angle  $\phi_r$  were calculated, and the results are plotted in Fig. 7, together with the results for films of other thicknesses, as a function of the film thickness. It is seen that the quantum efficiency decreases as the film thickness increases and becomes nearly constant for film

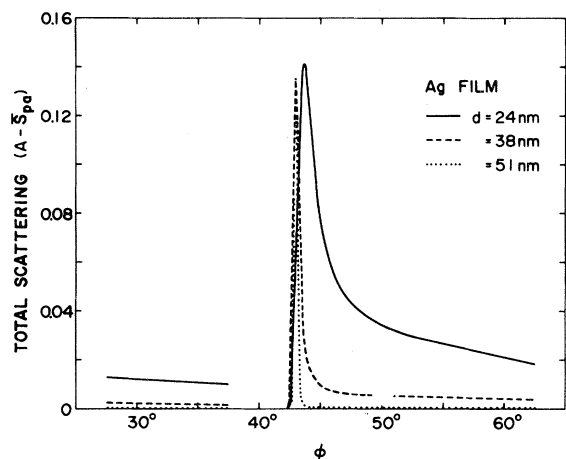


FIG. 6. Total scattering ( $A - \bar{S}_{pa}$ ) from silver films of different thickness  $d$  as a function of the angle of incidence  $\phi$ .

thicknesses  $\geq 40$  nm. We will find in the next section that this behavior of the quantum efficiency is, in general, consistent with the prediction of Kröger and Kretschmann's theory, which is plotted in Fig. 7 by a solid line.

As was mentioned in the first section of this paper, the radiative quantum efficiency determined here is from the plasmons which were scattered by the surface roughness. It is expected, therefore, that quantitative information concerning the roughness in our silver films may be extracted from the experimental results. Before trying to do this, we present

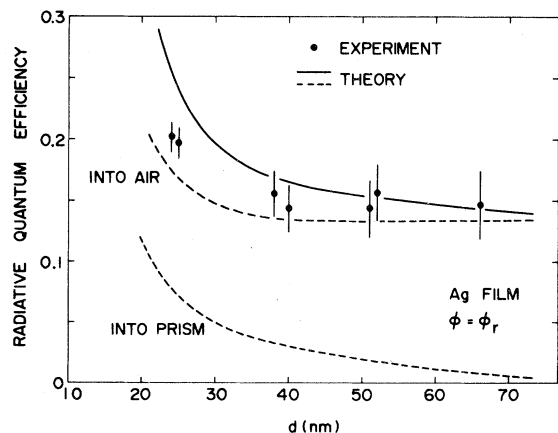


FIG. 7. Quantum efficiency for light emission at the plasmon resonance angle  $\phi_r$  as a function of film thickness  $d$ . Solid line represents the results calculated from the theory of Kröger and Kretschmann. Dashed lines represent theoretical contributions from light emission into the air and prism sides of film.

another set of experimental results obtained with silver films of variable surface roughness, which will further confirm the validity of the procedure used in data analysis.

### B. Silver films of variable roughness

In Fig. 8 we present the experimental results of the absorptance and the photoacoustic signal obtained for three 45-nm-thick silver films of different roughnesses as a function of the angle of incidence  $\phi$ . These differently roughened and equally thick silver films were made in the same evaporation onto  $\text{CaF}_2$  underlayers of different thicknesses which were evaporated onto a glass prism. It is seen that with increase of the underlayer thickness or the surface roughness, the plasmon resonance peak of the absorptance curve shifts to larger angles of incidence and the halfwidth becomes wider, indicating, respectively, that the plasmons become slow in propagation and rapid in decay due to interaction with the increasing roughness.<sup>15</sup> The absorptance

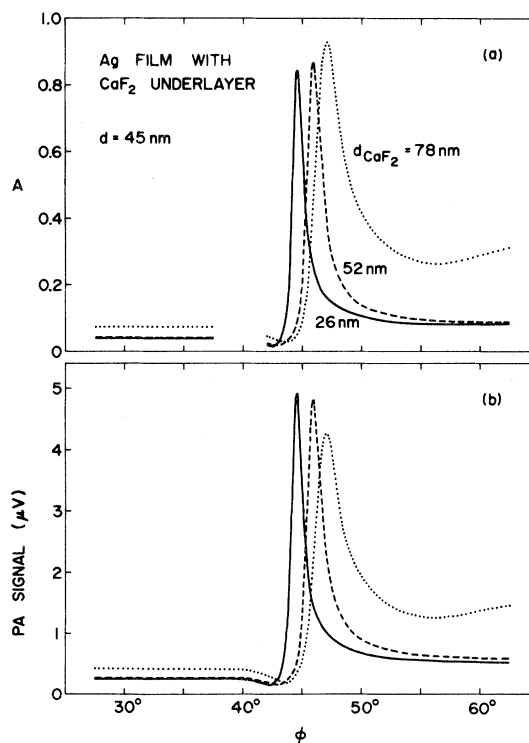


FIG. 8. (a) Absorptances  $A$  and (b) photoacoustic signal for three 45-nm-thick silver films roughened by  $\text{CaF}_2$  underlayers of different thicknesses  $d_{\text{CaF}_2}$  as a function of the angle of incidence  $\phi$ .

value increases only slightly at the plasmon peak, while it increases considerably at angles outside the resonance region as the underlayer thickness varies from 52 to 78 nm. These systematic changes of the absorptance values as a function of the underlayer thickness are similar to the behavior of the photoacoustic signal, except for differences in the plasmon peak heights. Contrary to the absorptance data, the peak height of the photoacoustic data decreases as the thickness of underlayer increases. This clearly demonstrates a contribution to the radiative decay which increases with increasing surface roughness.

The total light scattering ( $A - \bar{S}_{pa}$ ) of the roughened silver films obtained in the same manner as illustrated in Fig. 5 are presented in Fig. 9 as a function of the angle of incidence. The resultant radiative quantum efficiencies at the plasmon resonance angle  $\phi_r$  are plotted in Fig. 10 as a function of the  $\text{CaF}_2$  underlayer thickness. It is seen that the light scattering in the resonance region and the quantum efficiency both increase with increasing underlayer thickness. This shows that the absolute and the relative numbers of plasmons which enter the radiative decay channels both increase with increasing surface roughness. We do not know of any previous experimental data which can be compared directly with these experimental results. However, these results are consistent with the existing knowledge<sup>10</sup> concerning the behavior of surface plasmons on rough metal surfaces.

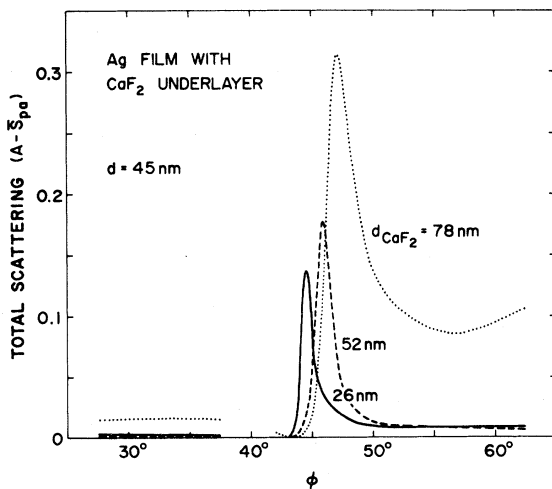


FIG. 9. Total scattering ( $A - \bar{S}_{pa}$ ) from three 45-nm-thick silver films roughened by  $\text{CaF}_2$  underlayers of different thicknesses  $d_{\text{CaF}_2}$  as a function of the angle of incidence  $\phi$ .

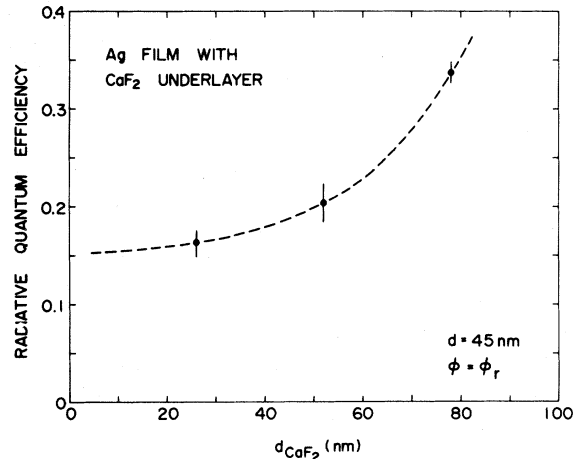


FIG. 10. Quantum efficiency for light emission at the plasmon resonance angle  $\phi_r$  for 45-nm-thick silver films roughened by  $\text{CaF}_2$  underlayer as a function of the underlayer thickness  $d_{\text{CaF}_2}$ .

In the present interpretation of the experimental data, we have ignored the effects of surface roughness and the  $\text{CaF}_2$  underlayer on the observed photoacoustic signal generation. The root-mean-square roughnesses of our silver films are, however, of the order of 1 nm; and at the present chopping frequency, they are smaller than the typical thermal diffusion length in our photoacoustic system by a factor of  $10^5$ . Also, the thermal properties and the density of  $\text{CaF}_2$  do not differ much from those of the glass prism on which the  $\text{CaF}_2$  was evaporated. Therefore, neither the surface roughness nor the underlayer are likely to cause any significant effects which make it necessary to change the present interpretation.

Of interest in the quantum efficiencies presented in Fig. 10 is that the value extrapolated to the limit of zero underlayer thickness,  $\sim 0.15$ , is very close to the value that would be expected for a 45-nm-thick film from the experimental results of the thickness-dependent quantum efficiency presented in Fig. 7. This result, demonstrating the consistency between two sets of data presented here implies that the  $\text{CaF}_2$  underlayer produces surface roughness such that it adds its own roughness to that which already exists on the glass prism and the film itself. Such a superposition of different surface roughnesses is possible if the difference between the correlation lengths associated with each component roughness is so large that they do not interfere with each other. Now let us return to the thickness-dependent results presented in the preceding subsection and compare them with theoretical predictions.

#### IV. COMPARISON WITH THEORY

The total light scattering from thin silver films of different thicknesses was calculated by using Kröger and Kretschmann's theory<sup>9</sup> for light scattering from rough thin films. Their model, consisting of a smooth surface and surface-current sources, was proved to be theoretically equivalent to the first-order perturbation theory<sup>16</sup> which calculates the scattering at the rough surface from the exact boundary conditions and makes a perturbative treatment for the roughness. The theoretical expression given by this model is the light-scattering cross section<sup>17</sup> which can be immediately used to calculate the scattered intensity from a rough thin film for light at any incidence angle as a function of the polarization of the scattered light and the scattering angle on the back side of the film. Hence, it is suitable for the calculation of total scattering into the air side of our silver film as a function of the angle of incidence. For light scattering back into the incident side of the film, Simon and Guha<sup>7</sup> have modified the Kröger-Kretschmann expression by assuming that, for *p*-polarized light incident at the plasmon resonance angle, scattered light also has *p* polarization because it arises primarily from directionally scattered plasmons. They found that their modification gave results which were fairly consistent with the observed scattering cross sections. We have used their expression at all angles of incidence to calculate the total scattering into the prism side of our silver film.

The main purpose of the present calculation is to see how the present experimental results of the total light scattering obtained as a function of film thickness and the resultant quantum efficiencies are consistent with the predictions of the Kröger-Kretschmann theory and to extract quantitative information concerning the roughness in our silver films. For these purposes, we assumed that the roughness is Gaussian-correlated and the roughness spectrum  $S(k)$  is given by<sup>7,9</sup>

$$|S(k)|^2 = (1/4\pi)\sigma^2\delta^2\exp(-\sigma^2k^2/4),$$

using the root-mean-square roughness  $\delta$  and the correlation length  $\sigma$ , where  $\hbar k$  is the transfer momentum. For *p*-polarized light, the scattering cross section into each scattering angle into the air side of the film was calculated from the Kröger-Kretschmann expression by using the literature values<sup>18</sup> of the optical constants for silver at 1.96 eV and integrated over all polarization azimuths and

then integrated over the entire hemisphere. The integrated scattering intensity into the prism side of the film was also calculated similarly from the modified Kröger-Kretschmann expression, and the total scattering intensity obtained by summing up these scattering intensities was calculated as a function of the angle of incidence and the film thickness.

Values of the roughness parameters  $\delta$  and  $\sigma$  were found which gave the best simultaneous fit of the calculated results of the scattering intensities at  $\phi = 30^\circ$  and  $60^\circ$  and the quantum efficiencies at the plasmon resonance angle to the respective experimental data obtained as a function of the angle of incidence. At the plasmon resonance angle, it was found that the calculated value of the scattering intensity from a silver film of a given thickness is very sensitive to the values of the optical constant of silver used, whereas the quantum efficiency obtained by dividing the scattering intensity by the calculated absorptance is not. We, therefore, used the quantum efficiency, rather than the scattering intensity, for comparison with experimental data at the resonance angle. In this calculation of the quantum efficiency, however, the calculated values of the absorptance for relatively thin films were found to be consistently smaller than the observed values, and the difference increased as the film thickness decreased. We have tried several different literature values of the optical constants of silver, but this trend was found to be the same. We interpreted this to be due to significant light scattering into the glass prism from the thin films used in the experiments. As was shown by Simon and Guha,<sup>7</sup> light scattering back into the prism is mainly from plasmons scattered directionally by roughness which should otherwise decay into photons in the direction of the specular reflection. Hence, an increase of this light scattering in thin films makes the observed absorptance larger than the value calculated for a smooth film. A correction for this contribution was made on the calculated absorptance values for films of all thicknesses by using the calculated values of the scattering intensity into the prism.

The best simultaneous fit of the calculated results of three different data to the respective experimental results was found to be obtained for  $\delta = 3.3 \pm 0.2$  nm and  $\sigma = 200 \pm 20$  nm. This set of values yielded a fairly sharp minimum in the least-squares analysis of the calculated and experimental data as a function of film thickness. The scattering intensities  $A - \bar{S}_{pa}$  at  $\phi = 60^\circ$  calculated with these roughness parameters are plotted in Fig. 11 and compared



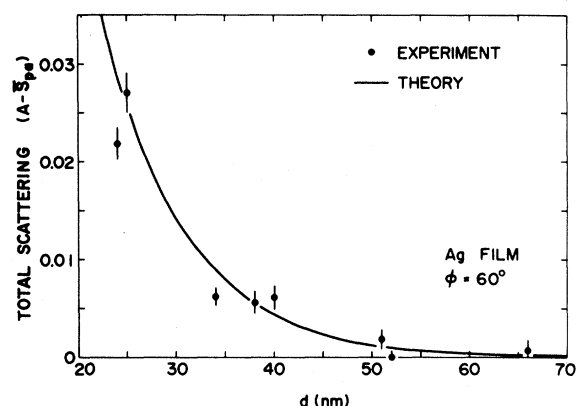


FIG. 11. Total scattering ( $A - \bar{S}_{pa}$ ) at the angle of incidence  $\phi = 60^\circ$  as a function of film thickness  $d$ . Solid line represents the results from Kröger and Kretschmann's theory.

with the experimental results. The scattering intensities at  $\phi = 30^\circ$  and the quantum efficiencies at the resonance angle  $\phi_r$ , calculated with the same roughness parameters have been presented in Figs. 4 and 7, respectively. The calculated results in each of these figures as a function of film thickness exhibit good quantitative agreement with the experimental data. The present experimental results of the light scattering as a function of the angle of photon incidence were thus found to be consistent with the predictions of the Kröger-Kretschmann theory for all film thicknesses studied.

The value of the root-mean-square roughness  $\delta$  determined above appears to be considerably larger than most of the previous values<sup>7,19,20</sup> for "smooth" silver films on glass or quartz substrates obtained by other experimental techniques. We believe that this was due to the surface quality of our prism substrate. Indeed, we observed for films deposited on a different glass prism the total light scattering  $A - \bar{S}_{pa}$ , which was consistently smaller than those presented in Fig. 6. This indicated that the prism surface used in this study did not have the best possible surface quality and was not as smooth as in the previous studies.

Using the values of  $\delta$  and  $\sigma$  determined above, we evaluated the quantum efficiencies for light emission from surface plasmons into the air and the prism sides separately and plotted them in Fig. 7 by dashed lines. The calculated efficiency into the air side is nearly constant for film thickness  $\geq 40$  nm, while the prism-side efficiency continues to decrease with film thickness and becomes considerably smaller than into the air side. This appears to be the reason for the difference between the previous

experimental results of the quantum efficiencies into the air and the prism sides of silver films obtained by Moreland *et al.*<sup>10</sup> and Simon and Guha,<sup>7</sup> respectively, from direct measurements of the emitted light.

## V. DISCUSSION AND SUMMARY

By using a combination of photoacoustic and optical measurements, we were able to determine the quantum efficiencies for light emission from surface plasmons excited in silver films of variable thickness and roughness. Surface plasmons which propagate along metal surfaces as polarization waves are believed to interact with the roughness quite efficiently and provide information which is difficult to obtain by other experimental probes. Hence, many attempts have been made to obtain quantitative information concerning roughness on metal surfaces by observing light emission from surface plasmons.<sup>7,20-22</sup> For relatively rough metal surfaces, diffuse light scattering has been utilized<sup>19,20</sup> also to study surface roughness. In either experiment, measurements are usually made on the angular distribution of scattered light, from which values of the roughness parameters are extracted by assuming a particular form of the roughness spectrum. In contrast to this, the present method measures the total light scattering integrated over all scattering angles. It is usually considered that total light scattering cannot provide enough information to give unique values of the roughness parameters. Indeed, we have found that, for the experimental results of the quantum efficiencies presented in Fig. 7 alone, for example, there is a wide range of roughness parameters which yield comparable best fits of the calculated data to the experimental data as a function of film thickness. The analysis made in the preceding section showed, however, that unique values of the roughness parameters can be obtained if total scattering is measured as a function of angle of incidence.

The present study also demonstrated that light scattering for incidence angles not only at the plasmon resonance angle but also at other angles ( $\phi = 30^\circ$ , for instance) is described by a single theoretical expression, given by Kröger and Kretschmann, by using a single set of values of the roughness parameters. This implies that light emission from surface plasmons and the usual diffuse light scattering from a rough surface yield consistent results on surface roughness. This has been expected<sup>20</sup> but has not been proved experimentally.

In conclusion, we have determined experimentally the total light scattering from thin silver films in an ATR geometry as a function of the angle of photon incidence by using the technique of combined photoacoustic and optical measurements. The quantum efficiencies for roughness-aided total light emission from surface plasmons were determined as a function of film thickness and roughness. Analysis of the results using a Gaussian roughness spectrum indicated consistency with the predictions of Kröger and Kretschmann's theory and gave a uniquely determined set of roughness parameters. The present study demonstrates the capability of

our photoacoustic technique as a tool for quantitative study of the relaxation process and its usefulness in surface study.

#### ACKNOWLEDGMENTS

This research was sponsored in part by the Great Lakes Colleges Association, Associated Colleges of the Midwest and the Office of Health and Environmental Research, U.S. Department of Energy, under Contract No. W-7405-eng-26 with the Union Carbide Corporation.

\*Present address: St. Olaf College, Northfield, MN 55057.

<sup>1</sup>T. Inagaki, K. Kagami, and E. T. Arakawa, *Phys. Rev. B* **24**, 3644 (1981).

<sup>2</sup>T. Inagaki, K. Kagami, and E. T. Arakawa, *Appl. Opt.* **21**, 949 (1982).

<sup>3</sup>A. Rosencwaig, in *Optoacoustic Spectroscopy and Detection*, edited by Y. H. Pao (Academic, New York, 1977), p. 193.

<sup>4</sup>E. Kretschmann, *Z. Phys.* **241**, 313 (1971).

<sup>5</sup>A. Otto, *Z. Phys.* **216**, 398 (1968).

<sup>6</sup>See, for review, for example, H. Raether, *Excitation of Plasmons and Interband Transitions by Electrons* (Springer, Berlin, 1980), pp. 116–171; A. Otto, in *Optical Properties of Solids—New Developments*, edited by B. O. Seraphin (North-Holland, Amsterdam, 1976), Chap. 13.

<sup>7</sup>H. J. Simon and J. K. Guha, *Opt. Commun.* **18**, 391 (1976).

<sup>8</sup>W. H. Weber and C. F. Eagen, *Opt. Lett.* **4**, 236 (1979).

<sup>9</sup>E. Kröger and E. Kretschmann, *Z. Phys.* **237**, 1 (1970).

<sup>10</sup>J. Moreland, A. Adams, and P. K. Hansma, *Phys. Rev. B* **25**, 2297 (1982).

<sup>11</sup>A. Rosencwaig and A. Gersho, *J. Appl. Phys.* **47**, 64 (1976).

<sup>12</sup>F. A. McDonald and G. C. Wetsel, *J. Appl. Phys.* **49**, 2313 (1978).

<sup>13</sup>For example, R. Bruns and H. Raether, *Z. Phys.* **237**, 98 (1970); D. G. Hall and A. J. Braundmeier, *Opt. Commun.* **7**, 343 (1973); W. H. Weber and S. L. McCarthy, *Phys. Rev. B* **12**, 5643 (1975).

<sup>14</sup>S. Hayashi, T. Yamada, and H. Kanamori, *Opt. Commun.* **36**, 195 (1981).

<sup>15</sup>A. J. Braundmeier and E. T. Arakawa, *J. Phys. Chem. Solids* **35**, 517 (1974).

<sup>16</sup>For example, S. L. McCarthy and J. Lambe, *Appl. Phys. Lett.* **30**, 427 (1977); J. C. Tsang, J. R. Kirtley, and J. A. Bradley, *Phys. Rev. Lett.* **43**, 772 (1979).

<sup>17</sup>E. Kretschmann, *Opt. Commun.* **5**, 331 (1972).

<sup>18</sup>P. B. Johnson and R. W. Christy, *Phys. Rev. B* **6**, 4370 (1972).

<sup>19</sup>For example, S. O. Sari, D. K. Cohen, and K. D. Scherkoske, *Phys. Rev. B* **21**, 2162 (1980); M. Rasigni and J. P. Palmari, *ibid.* **23**, 527 (1981); D. Beaglehole and O. Hunderi, *ibid.* **2**, 309 (1970); D. L. Hornauer, *Opt. Commun.* **16**, 76 (1976).

<sup>20</sup>J. Bodesheim and A. Otto, *Surf. Sci.* **45**, 441 (1974).

<sup>21</sup>E. Kretschmann, *Opt. Commun.* **10**, 353 (1974).

<sup>22</sup>D. G. Hall and A. J. Braundmeier, *Phys. Rev. B* **17**, 1557 (1978).